Studying the Supernova Absolute Magnitude Constancy with Baryonic Acoustic Oscillations

Denitsa Staicova[a,*]

[a1] Institute for Nuclear Research and Nuclear Energy, Bulgarian Academy of Sciences, Sofia, Bulgaria

E-mail: dstaicova@inrne.bas.bg

In this proceeding we review and expand on our recent work investigating the constancy of the absolute magnitude M_B of Type Ia supernovae. In it, we used baryonic acoustic oscillations (BAO) to calibrate the supernova data and to check whether the resulting M_B is constant. We used non-parametric methods like Gaussian processes and artificial neural networks to reconstruct $M_B(z)$. Here we elaborate on the results by putting them in the context of other studies investigating possible non-constant M_B and the impact of the distance-duality relation. We also present some numerical details on the calculations in the original paper and new non-parametric reconstructions, including a conservative model-independent fit, confirming its main results. Notably, we see that M_B remains constant within 1σ, with a possible jump around $z = 0.01 - 0.15$. Furthermore, the observed distribution of $M_B(z)$ cannot be described by a single Gaussian, displaying multiple peaks and tails. The choice of the only remaining parameter – the sound horizon r_d leads to a tension in the $M_B - r_d$ plane. Fitting different non-constant $M_B(z)$ models does not significantly improve the fit and there is no preference for any of the models by the statistical measures we employ.

*Speaker

1. Introduction

1.1 The tensions in cosmology

The study of supernovae type IA plays a major role in the cosmology. Observations of SNe Ia have demonstrated that the universe is expanding at an accelerated rate, described by the Hubble constant, H_0. However, when comparing the Hubble constant measured from the early universe and from the late universe, the two measurements deviate with more than 5σ [1–3] creating the so-called Hubble tension. This has led to a huge quest in improving both systematics and our numerical and theoretical models, but we see that there is no easy answer to the possible origin of the tension [4–18]. There are some hopeful candidates for resolving the H_0 tension, such as early dark energy models [19, 20] and interacting dark energy [21–24], but they still face challenges (for example resolving simultaneously the σ_8 tension [25, 26]).

Different studies have been performed trying to explain the Hubble tension. Among them, some have studied the possibility of a non-constant H_0 across different redshifts. For example, works using the redshift binned analysis on the SNe Ia Pantheon Sample ([18]) and a non-parametric approach on SNe, BAO and CC ([27]) have found evidence that H_0 decreases slowly with the redshift. A possible solution to the Hubble and growth tensions in the form of rapid transitions in G_{eff} have been also explored [28]. Intrinsic tension in the supernova sector of the local Hubble constant measurement have been discussed [29]. Ref. [30] has demonstrated that a cosmological underdensity cannot solve the Hubble tension. These are just few examples of the numerous works on the topic trying to solve the problem.

One way out of the situation is to look for an independent source of information such as the gravitational waves detectors. They, however, suffer for the moment from a low precision due to the small number of observed gravitational events accompanied by an electromagnetic counterpart and the associated big error box in the determination of the luminosity distance to the source and its redshift. For example, [31] measured from GW170814 and GW170817 $H_0 = 69^{+16}_{-18} km/s/Mpc$, while [32] published a reanalysis of GW170814 giving $H_0 \sim 75 km/s/Mpc$, [33] obtains from GW170817 and GW190814, $H_0 = 69^{+29}_{-14}$ km/s/Mpc. The inclusion of dark sirens (objects without EM counterpart) leads to the following results: $H_0 = 76.00^{+17.64}_{-13.45}$ km/s/Mpc for 10 well-localized dark sirens and GW170817 [34] and $H_0 = 72.77^{+11.0}_{-7.55}$ for 8 dark sirens and GW170817 [35]. Clearly, the precision is still far from the necessary for shining light on the Hubble tension. Other datasets like the GRB time-delays datasets might also be used to improve our understanding, but they would be relevant only in the case of evidence for non-zero Lorentz Invariance Violation [36].

Back to the standard objects we use in cosmology, one tries to build the distance ladder, starting from the closest objects (the Cepheids), through supernovae type IA (SNIA),[37, 38], cosmic chronometer [? ? ?], the baryonic acoustic oscillations (BAO) [39] and the cosmic microwave background [40]. When including BAO in our calculations, we face a well-known problem – the degeneracy between H_0, the sound horizon r_d and the matter density Ω_m. The sound horizon (r_d) is the distance at which the primordial sound waves that created BAO froze at recombination time and it's considered a known quantity. In BAO measurements, however, the sound horizon always appears coupled to H_0, i.e. as

the common factor $c/H_0 r_d$. This makes it impossible to find one of the quantities without calibrating the other with either the early or the late universe. There is also evidence that this degeneracy spreads also to the matter density Ω_m, leading to the so-called tension in the $H_0 - r_d - \Omega_m$ plane [41–44]. The coupling between the three parameters means that any solution of the H_0-tension should take into account also the other two parameters.

1.2 The supernova type IA mechanism

Supernovae type IA (SNe Ia) are essential tool in cosmology, since they are considered standard candles for distance measurements. These explosions originate from the thermonuclear disruption of white dwarf (WD) stars in binary systems, triggered when the mass of the WD reaches the Chandrasekhar limit of $1.4 M_\odot$. The limit mass gives them a stable peak luminosity and a characteristic broad, smooth light curve. The SNe Ia spectroscopy shows mostly carbon (C) and oxygen (O) lines, lack of hydrogen (H) and excess of silicon (Si).

To turn them into standard candles, one uses the distance modulus μ to connect the absolute SN magnitude M_B with the measured on Earth apparent magnitude m_B and the luminosity distance d_L trough:

$$\mu(z) = m_B(z) - M_B \tag{1}$$

$$m_B(z) - M_B = 5 log_{10}[d_L(z)/1Mpc] \tag{2}$$

Here, z is the redshift of the supernova and we have omitted the color and stretching corrections and the bias term for simplicity. The luminosity distance, accounting of the expansion of the universe, $H(z)$ trough:

$$d_L = (1 + z) \int_0^z \frac{cdz'}{H(z')} \tag{3}$$

The apparent magnitude is related to the observed flux in B-band at peak brightness F_B as

$$m_B \sim -2.5 log_{10}(F_B,)$$

while the observed flux depends on the emitted luminosity L at distance d_L as $F = L/4\pi d_L^2$.

The luminosity L is calculated through simulations based on theoretical models of the explosion mechanism and the composition of the white dwarfs. Since these models are well-established, the luminosity of a supernova is considered a known quantity, allowing their use as standard candles. However, there exist theories that may alter the Chandrasekhar limit but not the elemental composition, for example, for example magnetized WD, scalar-tensor theories, exotic particles and higher dimensions. Such theories would require reevaluation of the assumptions for calculating supernova luminosity.

Furthermore, since M_B is calibrated through nearby sample of objects with a known distance, it is considered a known constant. Few authors have suggested that taking a prior on M_B could replace the prior on H_0 [45, 46]. The idea is that this would avoid double counting of low-redshift supernovae and pre-setting the deceleration parameter, q_0 ([47]), and allowing to include the shape of the SNIa magnitude-redshift relation.

1.3 The constancy of M_B put in a context

The question of whether M_B is a constant for SNe Ia has been explored by numerous authors. Ref. [48, 49] developed models in which M_B would show a jump at $d \sim 20-50$Mpc. Ref. [50] finds that the SNe Ia from star-forming galaxies have different mean absolute magnitude ($M_B = -19.20 \pm 0.05$ mag) than those from passive elliptical galaxies ($M_B = -18.57 \pm 0.24$ mag). Additionally, Ref. [51] calibrated SN with BAO using the distance duality relation and a theoretical anchor to get $M_B(z = 2.34) - M_B(z = 0.32) = -0.08 \pm 0.15$. Ref.[52, 53] proposed as a resolution of the Hubble tension, a model with a transition at redshift $z_t < 0.1$ which performs better statistically than smooth late-time $H(z)$ deformation models.

The constancy of M_B relies essentially on the distance duality relation (Etherington's reciprocity theorem) or DDR. This relation states that the luminosity distance, $d_L(z)$, and the angular diameter distance, $d_A(z)$, are related by $d_L(z) = (1 + z)^2 d_A(z)$. This relation should hold for any metric theories of gravity where the photon number is conserved and light travels along null geodesics. The validity of DDR has been studied and confirmed in numerous contexts, but some signs for its violation have come from theories with curvature or dust, also dynamical dark energy, gravitational lensing, dust extinction, modified gravity, inhomogeneities, and clustering ([54–59]). These studies emphasize the importance of ongoing research of the constancy of M_B and its underlying assumptions.

2. The calibration of SN with BAO

In this proceeding, we review [4] in which we tested the constancy of M_B by calibrating SN measurements with BAO using a non-parametric (NP) approach. While we confirm that M_B remains constant within 1σ, there is an evidence of a possible jump in its value around $z = 0.01 - 0.15$ and signs of decreasing M_B for high z. Below, we summarize our approach and our results and offer new details on it.

2.1 Theoretical setup

The main idea of the approach is that having the observational data on SN and BAO, we can reconstruct in a non-parametric way the functional dependence $\mu(z)$ and $D_A/r_d(z)$ and then to use it to find M_B. The only remaining parameter in the problem is the sound horizon r_d, which we can set to either the early universe value or the late one. The formula we use to obtain M_B comes from Eq. 2 in which we have used the distance-duality relation to substitute the luminosity distance (d_L) obtained from the SN data with the angular diameter distance obtained from the BAO (D_A):

$$M_B = \mu_{Ia} - 5 \log_{10} \left[(1 + z)^2 \left(\frac{D_A}{r_d} \right)_{\text{BAO}} \cdot r_d \right] - 25 \,. \tag{4a}$$

For the theoretical uncertainty we obtain:

$$\Delta M_B = \Delta \mu_{Ia} + \frac{5}{\ln 10} \left[\frac{\Delta r_d}{r_d} + \frac{\Delta (D_A/r_d)_{BAO}}{(D_A/r_d)_{BAO}} \right] \,. \tag{4b}$$

where the Δ quantities refer to the observational uncertainties. This analytical formula is obtained by simplified error propagation which tends to overestimate the error (compared to the standard deviations error propagation).

In order to use this formula, we need to be able to reconstruct both $\mu_{Ia}(z)$ and $\frac{D_A}{r_d}$. This has to be done in a model-independent way, so that that we do not introduce further tension in our results.

2.2 The non-parametric approach

We consider two ways to perform a non-parametric fit of the data summarized below.

1. The Gaussian processes

GP reconstructs the dataset as part of a stochastic process in which each element is part of a multivariant normal distribution. It is defined via mean function $\mu(z)$ and a kernel function $k(z, z_1)$ and utilizes a Bayesian approach to optimize its kernel hyperparameters (σ_f and l). The GP is considered model-independent since it does not depend on the cosmological parameters, but only on the choice of the kernel. It has been tested in numerous cosmological studies, thus it is considered a robust way to make a model-independent fit. Its biggest advantage is that it naturally includes the errors of the measurements in the resulting fit.

As kernels we consider the Radial Basis (RB) function kernel and the Rational Quadratic (RQ) kernel:

$$k(z, \tilde{z})^{RB} = \sigma_f^2 \exp\left(-\frac{(z-\tilde{z})^2}{2l^2}\right), k(z, \tilde{z})^{RQ} = \frac{\sigma_f^2}{\left(1 + |z-z'|^2/2\alpha l^2\right)^{\alpha}}. \tag{5}$$

Additionally, here we show data for a third kernel – the Mattern kernel:

$$k(x_i, x_j) = \frac{1}{\Gamma(\nu)2^{\nu-1}}\left(\frac{\sqrt{2\nu}}{l}|z-z'|\right)^{\nu} K_{\nu}\left(\frac{\sqrt{2\nu}}{l}|z-z'|\right) \tag{6}$$

where $\Gamma(\nu)$ is the Gamma function of ν, $|z-z'|$ is the Euclidean distance between z and z' and $K_{(\nu)}$ is the Modified Bessel function of the second kind with order ν.

Examples of such GP reconstruction can be seen on Fig. 1. On it, we present different kernels with the same sound horizon $r_d = 153$Mpc. Adding other values of the sound horizon merely shift up and down the final result, since it enters as a constant, so we do not show this here. We can see that the interval on z can be split on 3 parts. At $z = 0$ we have a numeric singularity due to $D_A(z = 0) = 0$. More importantly however, we see that for small $z \sim 0.1 - 0.15$ we observe a jump in the values of M_B. It is unclear whether this is due to numerical issues or to the data fit. At large z we have big fluctuations due to GP becoming less certain because the BAO data points are fewer at these z. For this reason, we cut out plots at $z > 2$. However, there is a hint of decrease in the value of M_B for larger z. Finally, in the middle of the reconstruction ($z = 0.2 - 0.9$), we see that $M_B \sim const$ with no significant features in this interval.

2. Artificial Neural Networks (ANNs)

Another method to obtain a model-independent fit of the data is provided by ANNs. The ANN consists of input and output layers of neurons with a number of hidden layers of
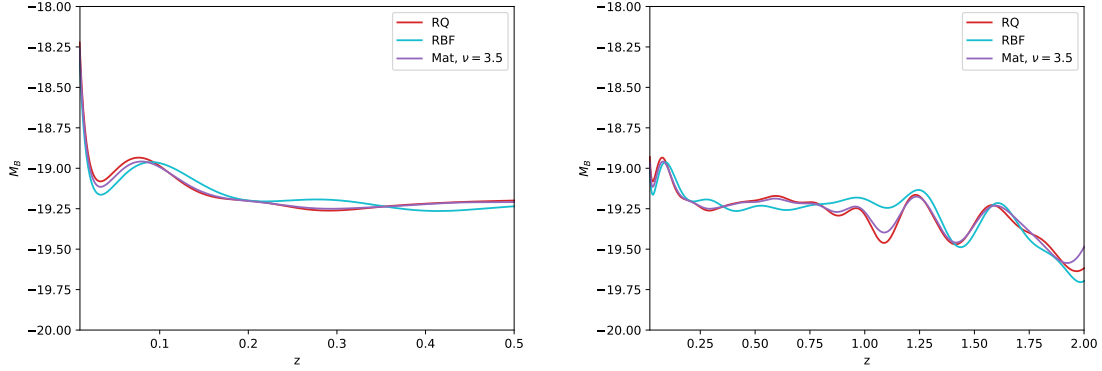
Figure 1: The reconstructed value for two of the kernels we used
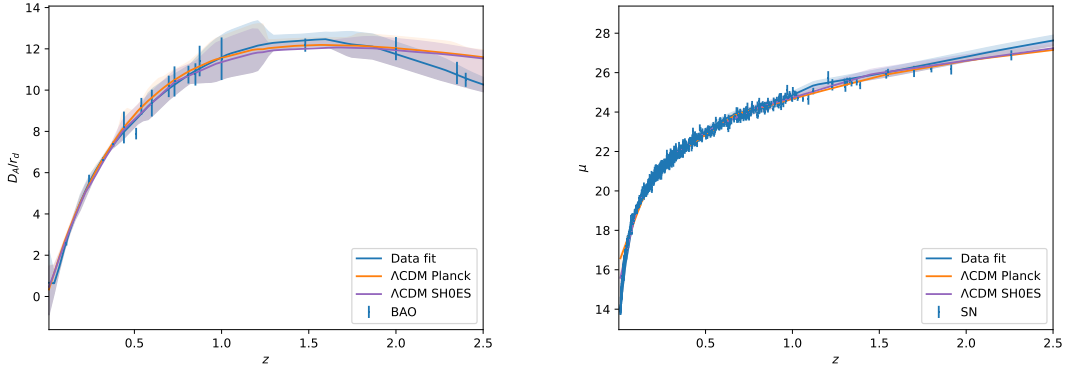
Figure 2: The ANN reconstruction of $D_A(z)/r_d$ and $\mu(z)$ plotted along with the observational data with its errors. The errors correspond to 1σ.

neurons, each connection having its weight. In our study, the input data are the redshifts and the output data are the observed quantities $(\mu(z), D_A/r_d(z)$ and their uncertainties. ANNs iteratively pass information forward and backward through their layers, adjusting their weights to minimize a loss function. During forward propagation, neurons in each layer compute weighted sums of inputs from connected neurons in the previous layer, followed by the application of an activation function. During the backpropagation step, the network computes gradients by propagating errors backward from the output layer to the input layer. These gradients are then used to re-adjust the weights to improve the fit. By optimizing the network's structure and parameters, ANNs provide a fit to the data without relying on specific model assumptions.

To train the ANN, we need to use mock datasets to find the optimal number of neurons and layers. In [4], the mock dataset mimics the redshift distribution of the real dataset and is generated by a risk-like statistic [60]. Furthermore, in this work we used the L1 loss function and a gradient–based optimizer based on Adam's algorithm [61] and the final ANN configuration is detailed in the paper.
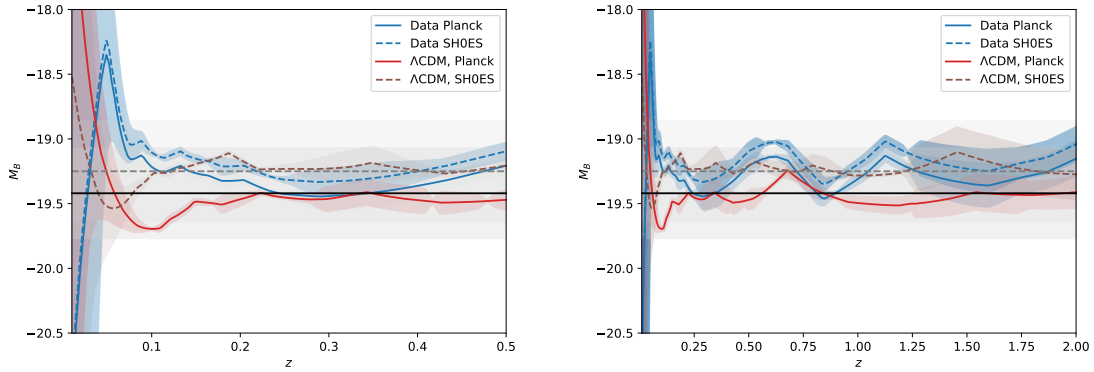
Figure 3: The ANN reconstruction of $D_A(z)/r_d$ and $\mu(z)$ for the two ΛCDM fits and the two data fits. The two horizontal lines correspond to the expected value for M_B for the SH0ES prior on H_0 (dashed) and the Planck one (solid)

On the Fig. 2 we show an example of reconstructions of $D_A(z)/r_d$ and $\mu(z)$ obtained in two cases – for mock data obtained from ΛCDM and from model-independent data fit (which we call "conservative approach"). In order to generate the mock data from ΛCDM, one needs to make an assumption for the cosmological parameters $[H_0, \Omega_m, r_d]$. Here in the Planck case we use $[67.4, 0.315, 147]$ [40], and for *SH0ES*: $[73.6, 0.26, 140.]$ [62], then one needs to add noise to the data. In the model-independent fit, we directly augment the data in a maximally conservative way (preserving the redshift distribution and the expected errors) and add noise.

From the figure, one can see that ΛCDM differs from the conservative fit and that the BAO data is much more sensitive to changes in it than the SN data. On the Fig. 3 we show the final reconstructions for M_B, similar to the ones obtained in [4]. On it we have presented four reconstructions, the two ΛCDM trained reconstructions that depend not-trivially on the sound horizon and the two trained on the conservative data-fit for which r_d is a mere constant (since it enters only in the final formula for M_B. The results are very similar to the GP ones, but much cleaner with respect to the over-all error. A small difference is that the ANN jump for small z is in the other direction. A notable result is that for ΛCDM-generated data, we have a significant area where the M_B is constant, while for the conservative approach, M_B is much more variable (since it follows closer the observational data). For all of the reconstructions, M_B increases for big z with the one from the conservative approach rising first. This differs from the obtained in [4] probably due to the different treatment of the training data. We have also zoomed at the beginning to demonstrate the jump seen for $z \in (0, 0.1]$. This jump has is present in all ANN reconstructions (as it is in the GP one) and it is in an interval where we have a lot of SN data points but very few BAO data points.

Finally, on fig. 4 we have summarized the results from both NP-reconstructions published in [4]. While the absolute magnitude remains constant within 1 σ, one can see that the reconstructed results do not follow a single Gaussian distribution but instead, they have

two peaks, or sometimes – tails. This have been shown on the figure by the mean values and the 1 σ errors for the obtained results. On this plot the index "fit" refers to the results being fitted to 2 Gaussians, while "Full" refers to the results being taken as a single Gaussian. We can see that the mean values are close to the expected from Planck and SH0ES only if one assumes a single Gaussian, otherwise - they are not. This can be seen also on Fig. 3 where even in the "constant" region, the reconstructions don't follow the "correct" horizontal line. Ref. [63] using the cosmographic approach got $M_B = -19.23 \pm 0.4$. Similar results have been published recently in [64] where the Pantheon+ dataset has been use to reconstruct M_B and again a shift in the nearby z region has been observed.
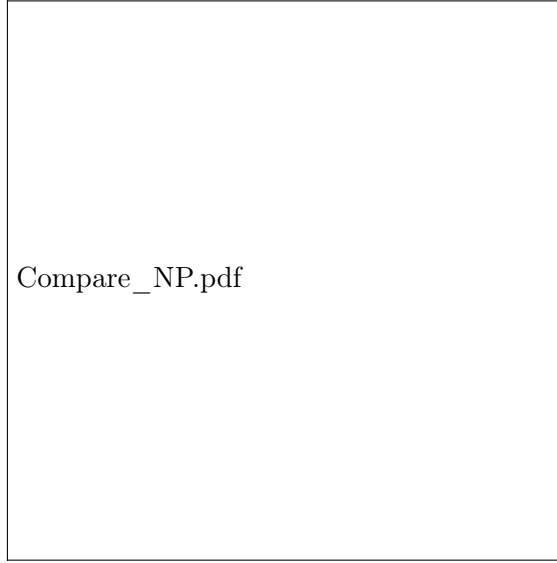
Figure 4: The comparison between the final mean values and their errors fro the different methods

2.3 Testing possible $M_B(z)$

To test different possible functional dependencies of $M_B(z)$ we test the following forms with a nested sampler provided by Polychord [65]. The goal is to check if any of these dependencies provides a better fit to the observational data, by minimizing $\chi^2 = \chi^2_{BAO} + \chi^2_{SN}$.

The functional forms for $M_B \rightarrow M_B + \delta M_B(z)$ we consider are [66, 67]:

$$\delta M_B(z) = \begin{cases} \epsilon z & \text{Model Line} \\ \epsilon \left[(1+z)^\delta - 1 \right] & \text{Model A} \\ \epsilon z^\delta & \text{Model B} \\ \epsilon \left[\ln(1+z) \right]^\delta & \text{Model C} \ . \end{cases} \tag{7}$$

We compare them with the default $M_B = const$ model on the background of the flat ΛCDM model.

Our test of possible color (C) and time stretching of the light curve (X_1) corrections in the SNIa light curves [68]:

$$\mu_{obs} = m^*_B - (M_B - \alpha X_1 + \beta C), \tag{8}$$
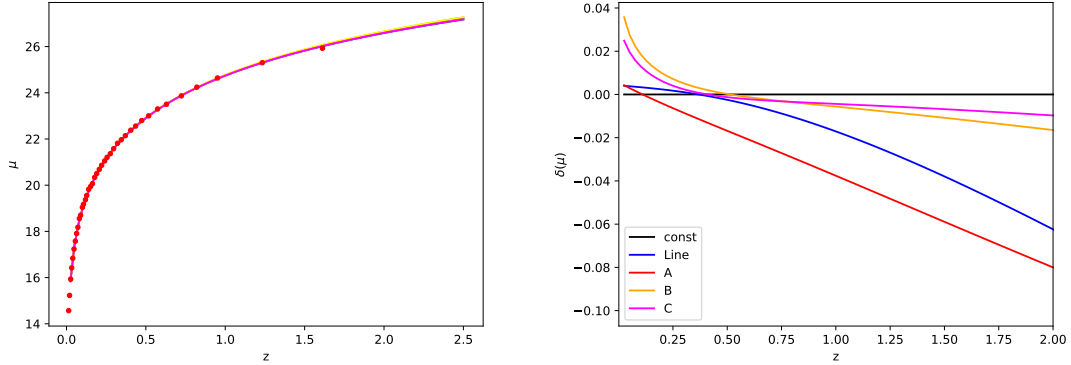
Figure 5: The posterior distribution for the nuisance parameters for different models with a ΛCDM background are shown, on the right panel corresponding to a prior $r_d^{Pl18} = 147.09 \pm 0.26$ Mp, on the left one - to $r_d^{HW+SN+BAO+SH0ES} = 136.1 \pm 2.7$ Mpc.

show that including the color and light curve stretching corrections as constants or as Gaussian priors, gives very similar results. Here α is the amplitude of the stretch correction and β - the amplitude of the color correction.

The priors we use to run the sampling are: uniform priors on H_0: $\in (50, 100)$, $\Omega_m \in (0.2, 0.4)$, $\Omega_r \in (0., 0.01)$, $\epsilon^{line} \in (-1, 1)$ and $\epsilon^{A,B,C} \in (-1, 1)$, $\delta \in (0, 1)$. The priors we use for α, X_1, β, C correspond to the G10 model in Ref. [69].

A summary of the results is that none of the tested model offers a convincing fit of the data. The statistical measures we tested and particularly the Bayesian factor do not confirm the dominance of one model. As a general behavior we find that unless we fix r_d, the system moves too freely in the $H_0 - r_d$ plane. On the other hand, fixing r_d is equivalent to fixing H_0 and moves the final results for M_B accordingly. Adding more parameters to the model increases the error but not significantly. On fig. 5, we see that the fits from the different models are practically indistinguishable with the current data points.

3. Conclusions and open questions

We have reviewed our recent work [4] in which we investigate the constancy of the absolute magnitude M_B of Type Ia supernovae by calibrating the SN data with BAO data. In order to obtain the dependency of the angular distance on the redshift corresponding to BAO data, we have used non-parametric methods like Gaussian processes and artificial neural networks (ANN). We have shown the comparison between Gaussian processes reconstructions and ANN ones, where for the ANN we have used model-dependent and model-independent ways to generate the training data.

The main result is that M_B remains constant within 1σ CL, but there is a deviation between the theoretically expected value for M_B and the reconstructed one. An interesting feature of our reconstructions is the possible jump around $z = 0.01 - 0.15$ that is seen in both NP methods we used. There is also possible evidence for an unexplained drift seen on high z that may be due to the higher error and the distribution of the BAO data.

Furthermore, the observed distribution of $M_B(z)$ cannot be described by a single Gaussian, indicating multiple peaks and tails. Despite excluding H_0 from our analysis, one still needs to fix r_d, which effectively replaces the $H_0 - r_d$ tensions with a tension in the $M_B - r_d$ plane. Fitting different non-constant $M_B(z)$ models does not significantly improve the fit, but also there is no preference for any of the models by the statistical measures we employ. The results of this work fit into the wider context of works examining the possibility of a non-constant M_B or a drift in H_0. It could also have a possible impact on the study of the distance-duality relation and its possible violation. Due to the particularities of the used non-parametric approaches, however, such study needs much more observational datapoints to be trustworthy in answering questions on the cosmological tensions.

Acknowledgments

References

[1] A.G. Riess, G.S. Anand, W. Yuan, S. Casertano, A. Dolphin, L.M. Macri et al., JWST Observations Reject Unrecognized Crowding of Cepheid Photometry as an Explanation for the Hubble Tension at 8σ Confidence, Astrophys. J. Lett. 962 (2024) L17 [2401.04773].

[2] E. Abdalla et al., Cosmology intertwined: A review of the particle physics, astrophysics, and cosmology associated with the cosmological tensions and anomalies, JHEAp 34 (2022) 49 [2203.06142].

[3] S. Vagnozzi, Seven Hints That Early-Time New Physics Alone Is Not Sufficient to Solve the Hubble Tension, Universe 9 (2023) 393 [2308.16628].

[4] D. Benisty, J. Mifsud, J. Levi Said and D. Staicova, On the robustness of the constancy of the Supernova absolute magnitude: Non-parametric reconstruction & Bayesian approaches, Phys. Dark Univ. 39 (2023) 101160 [2202.04677].

[5] M.G. Dainotti, B. De Simone, T. Schiavone, G. Montani, E. Rinaldi, G. Lambiase et al., On the Evolution of the Hubble Constant with the SNe Ia Pantheon Sample and Baryon Acoustic Oscillations: A Feasibility Study for GRB-Cosmology in 2030, Galaxies 10 (2022) 24 [2201.09848].

[6] B.L. Dias, F. Avila and A. Bernui, Probing cosmic homogeneity in the Local Universe, Mon. Not. Roy. Astron. Soc. 526 (2023) 3219 [2310.04594].

[7] K.F. Dialektopoulos, P. Mukherjee, J. Levi Said and J. Mifsud, Neural network reconstruction of scalar-tensor cosmology, Phys. Dark Univ. 43 (2024) 101383 [2305.15500].

[8] P.M.M. Alonso, C. Escamilla-Rivera and R. Sandoval-Orozco, *Constraining dark energy cosmologies with spatial curvature using Supernovae JWST forecasting*, 2309.12292.

[9] D. Benisty, A.-C. Davis and N.W. Evans, *Constraining Dark Energy from the Local Group Dynamics*, Astrophys. J. Lett. 953 (2023) L2 [2306.14963].

[10] K.F. Dialektopoulos, P. Mukherjee, J. Levi Said and J. Mifsud, *Neural network reconstruction of cosmology using the Pantheon compilation*, Eur. Phys. J. C 83 (2023) 956 [2305.15499].

[11] R. Briffa, C. Escamilla-Rivera, J. Levi Said and J. Mifsud, *Constraints on f(T) cosmology with Pantheon+*, Mon. Not. Roy. Astron. Soc. 522 (2023) 6024 [2303.13840].

[12] Y. Zhai, W. Giarè, C. van de Bruck, E. Di Valentino, O. Mena and R.C. Nunes, *A consistent view of interacting dark energy from multiple CMB probes*, JCAP 07 (2023) 032 [2303.08201].

[13] A. Bernui, E. Di Valentino, W. Giarè, S. Kumar and R.C. Nunes, *Exploring the H0 tension and the evidence for dark sector interactions from 2D BAO measurements*, Phys. Rev. D 107 (2023) 103531 [2301.06097].

[14] W. Yang, W. Giarè, S. Pan, E. Di Valentino, A. Melchiorri and J. Silk, *Revealing the effects of curvature on the cosmological models*, Phys. Rev. D 107 (2023) 063509 [2210.09865].

[15] S. Gariazzo, E. Di Valentino, O. Mena and R.C. Nunes, *Late-time interacting cosmologies and the Hubble constant tension*, Phys. Rev. D 106 (2022) 023530 [2111.03152].

[16] G. Bargiacchi, M.G. Dainotti, S. Nagataki and S. Capozziello, *Gamma-Ray Bursts, Quasars, Baryonic Acoustic Oscillations, and Supernovae Ia: new statistical insights and cosmological constraints*, 2303.07076.

[17] D. Staicova and M. Stoilov, *Electromagnetic Waves in Cosmological Spacetime*, Universe 9 (2023) 292.

[18] M.G. Dainotti, B. De Simone, T. Schiavone, G. Montani, E. Rinaldi and G. Lambiase, *On the Hubble constant tension in the SNe Ia Pantheon sample*, Astrophys. J. 912 (2021) 150 [2103.02117].

[19] V. Poulin, T.L. Smith, T. Karwal and M. Kamionkowski, *Early Dark Energy Can Resolve The Hubble Tension*, Phys. Rev. Lett. 122 (2019) 221301 [1811.04083].

[20] L. Herold and E.G.M. Ferreira, *Resolving the Hubble tension with early dark energy*, Phys. Rev. D 108 (2023) 043513 [2210.16296].

[21] S. Pan, W. Yang, E. Di Valentino, E.N. Saridakis and S. Chakraborty, Interacting scenarios with dynamical dark energy: Observational constraints and alleviation of the H_0 tension, Phys. Rev. D 100 (2019) 103520 [1907.07540].

[22] E. Di Valentino, A. Melchiorri, O. Mena, S. Pan and W. Yang, Interacting Dark Energy in a closed universe, Mon. Not. Roy. Astron. Soc. 502 (2021) L23 [2011.00283].

[23] E. Di Valentino, O. Mena, S. Pan, L. Visinelli, W. Yang, A. Melchiorri et al., In the realm of the Hubble tension—a review of solutions, Class. Quant. Grav. 38 (2021) 153001 [2103.01183].

[24] D. Benisty, S. Pan, D. Staicova, E. Di Valentino and R.C. Nunes, Late-Time constraints on Interacting Dark Energy: Analysis independent of H_0, r_d and M_B, 2403.00056.

[25] V. Poulin, J.L. Bernal, E.D. Kovetz and M. Kamionkowski, Sigma-8 tension is a drag, Phys. Rev. D 107 (2023) 123538 [2209.06217].

[26] V. Poulin, T.L. Smith and T. Karwal, The Ups and Downs of Early Dark Energy solutions to the Hubble tension: A review of models, hints and constraints circa 2023, Phys. Dark Univ. 42 (2023) 101348 [2302.09032].

[27] X.D. Jia, J.P. Hu and F.Y. Wang, Evidence of a decreasing trend for the Hubble constant, Astron. Astrophys. 674 (2023) A45 [2212.00238].

[28] V. Marra and L. Perivolaropoulos, Rapid transition of Geff at zt≃0.01 as a possible solution of the Hubble and growth tensions, Phys. Rev. D 104 (2021) L021303 [2102.06012].

[29] R. Wojtak and J. Hjorth, Intrinsic tension in the supernova sector of the local Hubble constant measurement and its implications, Mon. Not. Roy. Astron. Soc. 515 (2022) 2790 [2206.08160].

[30] S. Castello, M. Högås and E. Mörtsell, A cosmological underdensity does not solve the Hubble tension, JCAP 07 (2022) 003 [2110.04226].

[31] LIGO Scientific, Virgo, VIRGO collaboration, A Gravitational-wave Measurement of the Hubble Constant Following the Second Observing Run of Advanced LIGO and Virgo, Astrophys. J. 909 (2021) 218 [1908.06060].

[32] A. Palmese, R. Kaur, A. Hajela, R. Margutti, A. McDowell and A. MacFadyen, A standard siren measurement of the Hubble constant using GW170817 and the latest observations of the electromagnetic counterpart afterglow, 2305.19914.

[33] S. Vasylyev and A. Filippenko, A Measurement of the Hubble Constant using Gravitational Waves from the Binary Merger GW190814, Astrophys. J. 902 (2020) 149 [2007.11148].

[34] V. Alfradique et al., A dark siren measurement of the Hubble constant using gravitational wave events from the first three LIGO/Virgo observing runs and DELVE, 2310.13695.

[35] A. Palmese, C.R. Bom, S. Mucesh and W.G. Hartley, A Standard Siren Measurement of the Hubble Constant Using Gravitational-wave Events from the First Three LIGO/Virgo Observing Runs and the DESI Legacy Survey, Astrophys. J. 943 (2023) 56 [2111.06445].

[36] D. Staicova, Probing for Lorentz Invariance Violation in Pantheon Plus Dominated Cosmology, Universe 10 (2024) 75 [2401.06068].

[37] A.G. Riess et al., A Comprehensive Measurement of the Local Value of the Hubble Constant with 1 km s^{-1} Mpc^{-1} Uncertainty from the Hubble Space Telescope and the SH0ES Team, Astrophys. J. Lett. 934 (2022) L7 [2112.04510].

[38] A.G. Riess, S. Casertano, W. Yuan, L.M. Macri and D. Scolnic, Large Magellanic Cloud Cepheid Standards Provide a 1% Foundation for the Determination of the Hubble Constant and Stronger Evidence for Physics beyond ΛCDM, Astrophys. J. 876 (2019) 85 [1903.07603].

[39] eBOSS collaboration, Completed SDSS-IV extended Baryon Oscillation Spectroscopic Survey: Cosmological implications from two decades of spectroscopic surveys at the Apache Point Observatory, Phys. Rev. D 103 (2021) 083533 [2007.08991].

[40] Planck collaboration, Planck 2018 results. VI. Cosmological parameters, Astron. Astrophys. 641 (2020) A6 [1807.06209].

[41] L. Knox and M. Millea, Hubble constant hunter's guide, Phys. Rev. D 101 (2020) 043533 [1908.03663].

[42] D. Staicova, Hints for the H0 — rd tension in uncorrelated Baryon Acoustic Oscillations dataset, in 16th Marcel Grossmann Meeting on Recent Developments in Theoretical and Experimental General Relativity, Astrophysics and Relativistic Field Theories, 11, 2021, DOI [2111.07907].

[43] D. Staicova, DE Models with Combined $H_0 \cdot r_d$ from BAO and CMB Dataset and Friends, Universe 8 (2022) 631 [2211.08139].

[44] D. Staicova, Model selection results from different BAO datasets – DE models and Ω_KCDM, PoS CORFU2022 (2023) 188 [2303.11271].

[45] G. Efstathiou, To H0 or not to H0?, Mon. Not. Roy. Astron. Soc. 505 (2021) 3866 [2103.08723].

[46] D. Camarena and V. Marra, On the use of the local prior on the absolute magnitude of Type Ia supernovae in cosmological inference, Mon. Not. Roy. Astron. Soc. 504 (2021) 5164 [2101.08641].

[47] A.G. Riess et al., A 2.4% Determination of the Local Value of the Hubble Constant, Astrophys. J. 826 (2016) 56 [1604.01424].

[48] L. Perivolaropoulos and F. Skara, A Reanalysis of the Latest SH0ES Data for H_0: Effects of New Degrees of Freedom on the Hubble Tension, Universe 8 (2022) 502 [2208.11169].

[49] L. Perivolaropoulos and F. Skara, On the homogeneity of SnIa absolute magnitude in the Pantheon+ sample, Mon. Not. Roy. Astron. Soc. 520 (2023) 5110 [2301.01024].

[50] C. Ashall, P. Mazzali, M. Sasdelli and S. Prentice, Luminosity distributions of Type Ia Supernovae, Mon. Not. Roy. Astron. Soc. 460 (2016) 3529 [1605.05507].

[51] J. Evslin, Calibrating Effective Ia Supernova Magnitudes using the Distance Duality Relation, Phys. Dark Univ. 14 (2016) 57 [1605.00486].

[52] G. Alestas, L. Kazantzidis and L. Perivolaropoulos, $w - M$ phantom transition at z_t <0.1 as a resolution of the Hubble tension, Phys. Rev. D 103 (2021) 083517 [2012.13932].

[53] G. Alestas, D. Camarena, E. Di Valentino, L. Kazantzidis, V. Marra, S. Nesseris et al., Late-transition versus smooth $H(z)$-deformation models for the resolution of the Hubble crisis, Phys. Rev. D 105 (2022) 063538 [2110.04336].

[54] F. Renzi, N.B. Hogg and W. Giarè, The resilience of the Etherington–Hubble relation, Mon. Not. Roy. Astron. Soc. 513 (2022) 4004 [2112.05701].

[55] J. Qin, F. Melia and T.-J. Zhang, Test of the cosmic distance duality relation for arbitrary spatial curvature, Mon. Not. Roy. Astron. Soc. 502 (2021) 3500 [2101.05574].

[56] M.-Z. Lyu, Z.-X. Li and J.-Q. Xia, Testing the Cosmic Distance Duality Relation with the Latest Strong Gravitational Lensing and Type Ia Supernovae, Astrophys. J. 888 (2020) 32.

[57] Y. He, Y. Pan, D.-P. Shi, S. Cao, W.-J. Yu, J.-W. Diao et al., Cosmological-model-independent tests of cosmic distance duality relation with Type Ia supernovae and radio quasars, Chin. J. Phys. 78 (2022) 297 [2206.04946].

[58] C. Ma and P.-S. Corasaniti, Statistical Test of Distance–Duality Relation with Type Ia Supernovae and Baryon Acoustic Oscillations, Astrophys. J. 861 (2018) 124 [1604.04631].

[59] X. Fu and P. Li, Testing the distance–duality relation from strong gravitational lensing, type Ia supernovae and gamma-ray bursts data up to redshift $z \sim 3.6$, Int. J. Mod. Phys. D 26 (2017) 1750097 [1702.03626].

[60] PICA Group collaboration, Non-parametric inference in astrophysics, astro-ph/0112050.

[61] D.P. Kingma and J. Ba, Adam: A Method for Stochastic Optimization, arXiv e-prints (2014) arXiv:1412.6980 [1412.6980].

[62] D. Brout et al., The Pantheon+ Analysis: Cosmological Constraints, Astrophys. J. 938 (2022) 110 [2202.04077].

[63] D. Camarena and V. Marra, Local determination of the Hubble constant and the deceleration parameter, Phys. Rev. Res. 2 (2020) 013028 [1906.11814].

[64] P. Mukherjee, K.F. Dialektopoulos, J. Levi Said and J. Mifsud, Late-time transition of M_B inferred via neural networks, 2402.10502.

[65] W.J. Handley, M.P. Hobson and A.N. Lasenby, PolyChord: nested sampling for cosmology, Mon. Not. Roy. Astron. Soc. 450 (2015) L61 [1502.01856].

[66] I. Tutusaus, B. Lamine, A. Dupays and A. Blanchard, Is cosmic acceleration proven by local cosmological probes?, Astron. Astrophys. 602 (2017) A73 [1706.05036].

[67] S. Linden, J.-M. Virey and A. Tilquin, Cosmological Parameter Extraction and Biases from Type Ia Supernova Magnitude Evolution, Astron. Astrophys. 50 (2009) 1095 [0907.4495].

[68] R. Tripp, A Two-parameter luminosity correction for type Ia supernovae, Astron. Astrophys. 331 (1998) 815.

[69] Pan-STARRS1 collaboration, The Complete Light-curve Sample of Spectroscopically Confirmed SNe Ia from Pan-STARRS1 and Cosmological Constraints from the Combined Pantheon Sample, Astrophys. J. 859 (2018) 101 [1710.00845].

PoS(CORFU2023)180